

INTRAMOLECULAR EXCIMER FORMATION IN 2-(1-NAPHTHYL)-ETHYL 1-NAPHTHYLMETHYL ETHER: KINETIC AND THERMODYNAMIC RESULTS

R. V. TODESCO[†]

Radiation Laboratory, University of Notre Dame, Notre Dame, IN 46556 (U.S.A.)

J. PUT

University Centre of Limburg, Universitaire Campus, B-3610 Diepenbeek (Belgium)

(Received December 10, 1985)

Summary

An analysis of the intramolecular excimer formation in 2-(1-naphthyl)-ethyl 1-naphthylmethyl ether (DNEME) was carried out, based on spectral data and time-dependent fluorescence intensities at different temperatures and wavelengths. The rate constants for formation and deactivation of the excimer and the values of ΔH and ΔS were determined, according to Förster's kinetic scheme. In addition to fluorescence and radiationless deactivation, the excimer underwent reaction to an endo cycloadduct. The differences in the excimer properties of DNEME, di(1-naphthylmethyl) ether and 1,4-di(1-naphthyl)butane were interpreted in terms of steric factors induced by the type of chain linking the two naphthyl chromophores.

1. Introduction

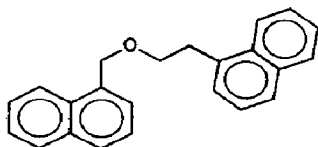
Intramolecular excimer formation and photocyclomerization have been investigated for a large number of bichromophoric systems containing naphthyl chromophores [1 - 15]. In dinaphthyl compounds containing a three-atom chain, temperature-dependent fluorescence spectra and lifetime measurements revealed the rather complex nature of intramolecular excimer formation in these systems [6, 9 - 12].

Itagaki *et al.* [9] observed dual excimer formation in the fluorescence spectra of 1,3-di[1-(4-methoxynaphthyl)]propane and 1,3-di[1-(4-hydroxynaphthyl)]propane. They ascribed this phenomenon to the existence of two different excimer geometries, caused by the bulky substituents and by intramolecular hydrogen-bond formation. For several 2-substituted dinaphthyl compounds a bi-exponential course for the excimer emission has

[†]On leave from the University Centre of Limburg, Belgium.

been reported [10, 11]. For *meso*- and *rac*-1,1'-di(1-naphthyl)-diethyl ether, De Schryver *et al.* [12] proved the existence of at least two excimers. Photocleavage of the formed exo cycloadducts revealed that the hypsochromic excimer in the *meso* compound had an exo configuration. These data were interpreted in terms of hindered rotation around the bond between the 1-naphthyl carbon and the methine carbon, in combination with steric interactions between the peri H_8, H_8 hydrogens and the methyl substituents. In a previous paper [6] we reported a kinetic scheme for intramolecular excimer formation in di(1-naphthylmethyl) ether, involving different starting conformations. We observed a direct correlation between the quantum yields of excimer emission in solution and the ratios of exo and endo cyclomers.

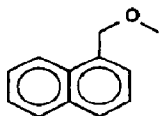
For dinaphthyl compounds with longer linking chains only fluorescence under stationary conditions and intramolecular photoreactivity have been studied up to now [1, 14] but no thermodynamic and kinetic data have been reported. For 1,4-di(1-naphthyl)butane, a weak excimer fluorescence at low temperatures was observed by Chandross and Dempster [1]. Davidson and Whelan [14] reported excimer formation in 2-(2-naphthyl)-ethyl 2-naphthylmethyl ether. For the 1-naphthyl analogue, however, neither excimer fluorescence nor cyclomerization was detected and the quantum yield of monomer fluorescence was found to be within 10% of that for the model compound methyl 1-naphthylmethyl ether. In this paper, we want to present a more extensive study of the intramolecular excimer formation and photocyclomerization of 2-(1-naphthyl)ethyl 1-naphthylmethyl ether (DNEME)



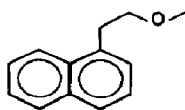
DNEME

in dilute iso-octane solution.

Fluorescence data under stationary and non-stationary conditions, in a temperature range from -80 to $+50$ °C, are presented. As model compounds, we used methyl 1-naphthylmethyl ether (NMME) and methyl 2-(1-naphthyl)ethyl ether (NEME):



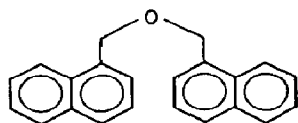
NMME



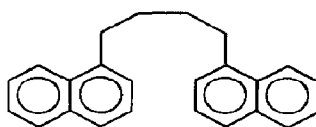
NEME

The effect of the linking chain on the photocyclomerization and on the spectral, kinetic and thermodynamic properties of the intramolecular excimer formation in DNEME is discussed in relation to the excimer formation

in di(1-naphthylmethyl) ether (DNME) and in 1,4-di(1-naphthyl)butane (DNB):



DNME



DNB

2. Experimental details

The syntheses of NMME and of DNEME were described in refs. 4 and 7 respectively.

2.1. Synthesis of methyl 2-(1-naphthyl)ethyl ether

To a solution of 0.24 g (10 mmol) NaH in 50 ml dry tetrahydrofuran (THF), 1.72 g (10 mmol) 2-(1-naphthyl)ethanol were added and stirred for 5 h at room temperature. 1.14 g (8 mmol) iodomethane were added slowly and the solution was stirred for an additional 24 h. The mixture was poured into 250 ml H₂O and extracted with toluene. A first purification was performed by column chromatography on silica gel with toluene. Preparative high performance liquid chromatography on silica gel (10 μm) with cyclohexane-CH₂Cl₂ (75:25 by volume), followed by Kugelrohr distillation at 90 °C and 0.1 mmHg, yielded 0.97 g (52% yield) of a colorless liquid. ¹H nuclear magnetic resonance (CDCl₃-TMS): δ = 3.42 ppm (singlet (s), -O-CH₃, 3 H); δ = 3.45 ppm (triplet (t), CH₃-O-CH₂CH₂, 2 H, J = 6 Hz); δ = 3.80 ppm (t, CH₃-O-CH₂CH₂, 2 H, J = 6 Hz); δ = 7.50 - 8.40 ppm (multiplet (m), aryl, 7 H). Elementary analysis was as follows: C, 83.81%; H, 7.59%; the calculated values for C₁₃H₁₄O₁ are 83.83% C and 7.58% H.

2.2. Solvents

Iso-octane, acetonitrile and 2-propanol were purchased from Merck (Uvasol) and were used without further purification. None of the solvents used seemed to contain fluorescent contaminants on excitation in the wavelength region of experimental interest.

2.3. Instrumentation

Absorption spectra were recorded using a Varian Techtron 635 or a Perkin-Elmer 124 double-beam spectrophotometer. Optical densities were measured using a Varian or a Hitachi spectrophotometer. Corrected emission spectra were run employing a Fica absolute and differential fluorometer and excitation spectra were run using a Spex Fluorolog. The temperature was controlled by a stream of nitrogen which was first passed through liquid nitrogen and then heated to the appropriate temperature. Decay measurements were performed by the single-photon counting technique

using apparatus composed of Ortec and Canberra modules and an optical system from Applied Photophysics. The observed decays were deconvoluted by using a lamp spectrum and a non-linear least-squares program. Reaction quantum yields were determined according to a method described in a previous paper [16].

3. Results

3.1. Absorption spectra

In Fig. 1 the UV absorption spectra of DNEME, NMME and NEME in iso-octane are compared. These absorption spectra show the same course in all three solvents studied, iso-octane, 2-propanol and acetonitrile. The wavelengths of the maxima are independent of the solvent. A close analysis of the spectra revealed that in DNEME the ${}^1L_a \leftarrow {}^1A$ band is very slightly shifted (1.5 nm) to bathochromic wavelengths compared with that of NMME. In contrast, DNEME shows a slight hypochromism between 240 and 296 nm and a slight hyperchromism between 240 and 310 nm compared with NEME and NMME respectively, but at longer wavelengths the spectra coincide. As a function of temperature (from -50 to $+50$ °C) no splitting of bands or shift occurred in any of the solvents. The only effect was an increase in vibronic structure at lower temperatures. It can be concluded that no strong interaction between the naphthalene chromophores in the ground state of DNEME exists in any solvent used.

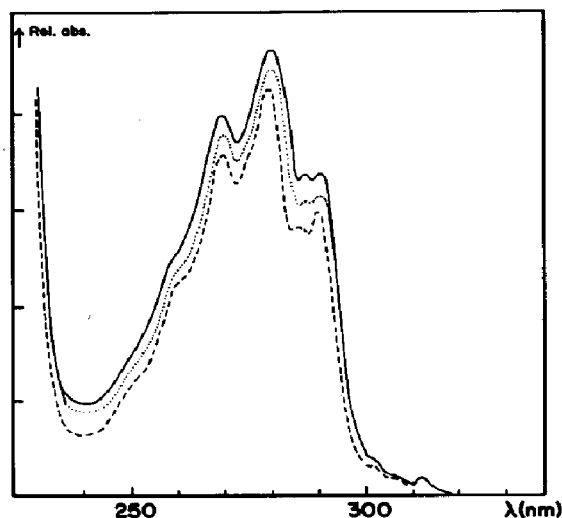


Fig. 1. Absorption spectra of DNEME (.....), NMME (---) and NEME (—) in iso-octane (10^{-5} M) at 293 K.

3.2. Fluorescence of the model compounds

The fluorescence spectra of NEME and NMME are typical for a locally excited 1-substituted naphthalene with maxima at 321 and 336 nm in

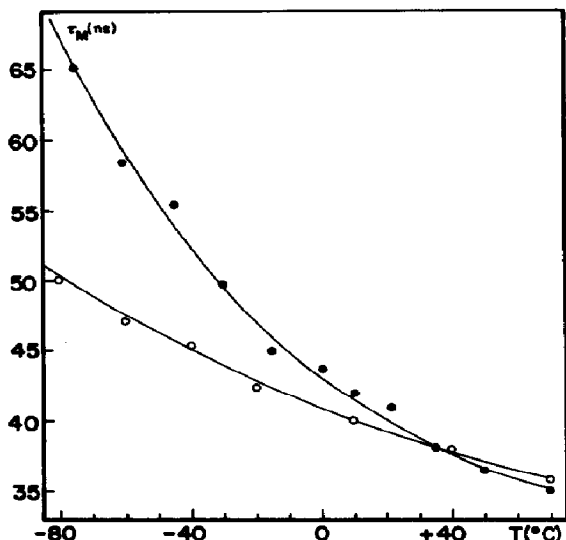


Fig. 2. Fluorescence lifetimes of NMME (○) and NEME (●) vs. temperature in iso-octane.

various solvents [6]. The lifetimes, obtained by the analysis of the mono-exponential decays at various temperatures, are plotted against temperature in Fig. 2. From the lifetime and the quantum yield at room temperature, the fluorescence rate constant k_{FM} was calculated and the value of k_{FM}^0 was obtained, with the refractive index taken into account [17, 18]. Relating $\ln k_{IM}$ (where k_{IM} is the rate constant for non-radiative decay) to $1/T$ yielded a straight line from which the activation energy E_{IM} of non-radiative decay was calculated. The values of the various photophysical constants of NEME and NMME at room temperature in iso-octane are summarized in Table 1.

TABLE 1

Photophysical constants of methyl 2-(1-naphthyl)ethyl ether and methyl 1-naphthyl-methyl ether in iso-octane at room temperature

Compound	ϕ_{FM}	τ (ns)	$10^7 k_{FM}$ (s^{-1})	$10^7 k_{FM}^0$ (s^{-1})	$10^7 k_{IM}$ (s^{-1})	$10^7 A_{IM}$ (s^{-1})	E_{IM} (kJ mol $^{-1}$)
NEME	0.090	41.0	0.22	0.11	2.2	6.9	2.7
NMME	0.080	38.8	0.23	0.12	2.4	4.0	1.5

3.3. Fluorescence of 2-(1-naphthyl)ethyl 1-naphthylmethyl ether under stationary conditions

The fluorescence spectra obtained in dilute solutions (10^{-4} M) of DNEME in iso-octane (Fig. 3), acetonitrile and 2-propanol at room temperature show emission from locally excited naphthalene and a broad

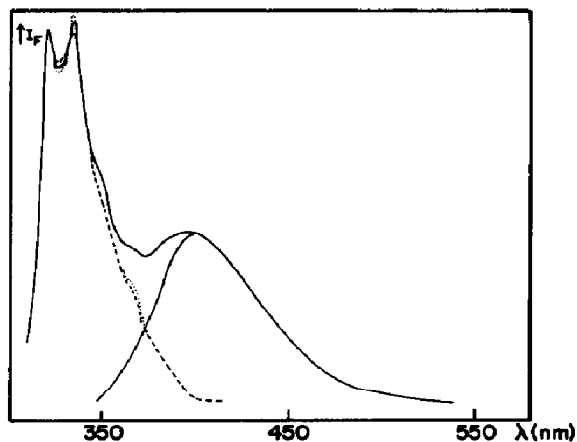


Fig. 3. Corrected emission spectra of DNEME (—), NMME (- - -) and NEME (.....) in iso-octane at 293 K ($\lambda_{\text{EXC}} = 290$ nm).

structureless emission attributed to an excimer. The structure and maximum of the excimer emission can be determined from difference spectra between DNEME and NEME or NMME, after normalization at the 0-0 transition. The position of the maximum is at 398 nm and is solvent independent but only slightly temperature dependent: in iso-octane the maximum of the excimer emission varies from 404 nm at -70°C to 395 nm at $+80^\circ\text{C}$. At 77 K in an ethanol matrix the fluorescence of DNEME is nearly identical with that of NEME and NMME. No excimer emission is detected, indicating that rotation is required for excimer formation (Fig. 4). The quantum yields of monomer and excimer emission at room temperature in the various solvents are summarized in Table 2.

In iso-octane, in the temperature region from -70 to -45°C , the monomer fluorescence decreases, whereas the excimer emission remains virtually constant. From -45°C on, the fluorescence spectra of DNEME show an isoemissive point near 363 nm and the decrease in excimer fluorescence is compensated for by an increase in the locally excited state (Fig. 5), which is indicative of dissociation of the excimer. Thus from -45°C on, a picture emerges similar to that for intermolecular excimer formation [19,

TABLE 2

Quantum yields of monomer emission (ϕ_{FM}), excimer emission (ϕ_{FD}) and their ratio ($\phi_{\text{FD}}/\phi_{\text{FM}}$) for 2-(1-naphthyl)ethyl 1-naphthylmethyl ether in some solvents at room temperature

Solvent	ϕ_{tot}	ϕ_{FM}	ϕ_{FD}	$\phi_{\text{FD}}/\phi_{\text{FM}}$
Iso-octane	0.090	0.044	0.046	1.05
Acetonitrile	0.085	0.048	0.037	0.77
2-Propanol	0.091	0.036	0.055	1.53

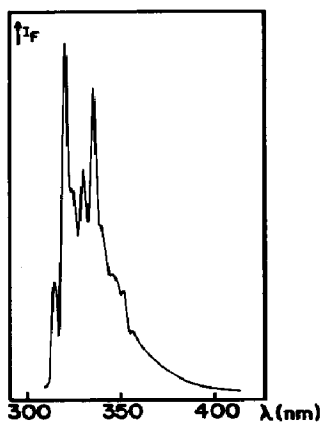


Fig. 4. Corrected emission spectrum of DNEME in an ethanol matrix at 77 K ($\lambda_{\text{EXC}} = 290$ nm).

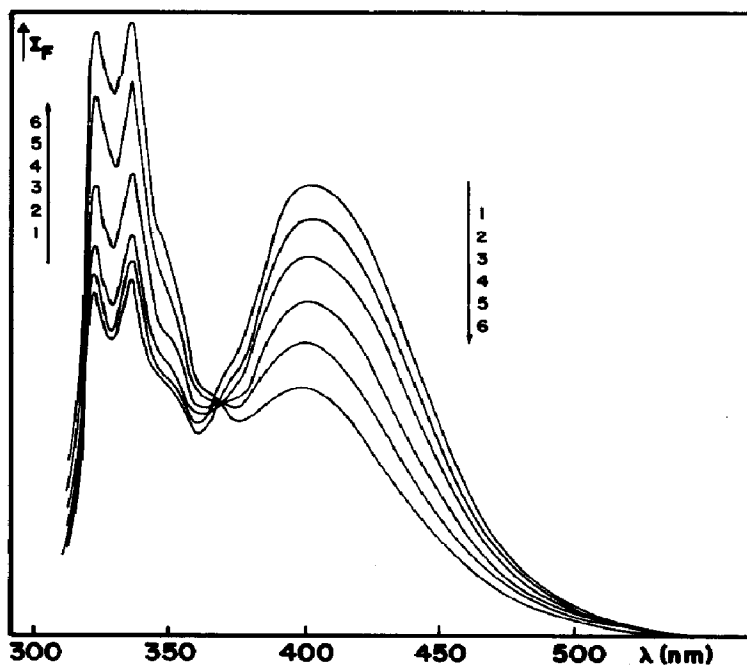


Fig. 5. Corrected fluorescence spectra of DNEME in iso-octane at various temperatures: curve 1, 228 K; curve 2, 241 K; curve 3, 253 K; curve 4, 268 K; curve 5, 283 K; curve 6, 296 K.

20]. A Stevens-Ban plot [19] generates a straight line at higher temperatures (Fig. 6). As an isoemissive point exists at these temperatures, the excimer stabilization energy ΔH can be obtained from the gradient of this line [21 - 24]. The low temperature region in the Stevens-Ban plot could not be reached.

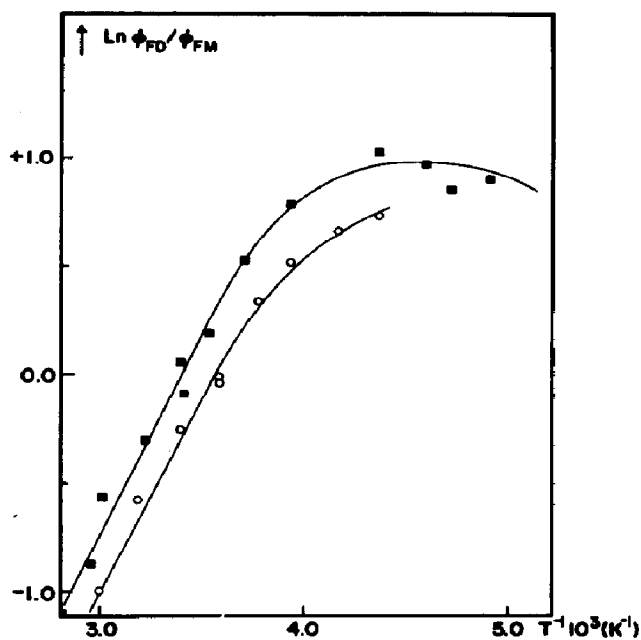


Fig. 6. Stevens-Ban plots of DNEME in iso-octane (■) and acetonitrile (○).

3.4. Fluorescence of 2-(1-naphthyl)ethyl 1-naphthylmethyl ether under non-stationary conditions

The time-dependent fluorescence intensities $I_M(t)$ (locally excited state) and $I_D(t)$ (excimer) were recorded at 330 nm and 450 nm respectively in iso-octane at various temperatures. The emission at 330 nm decays tri-exponentially (Fig. 7) between -70 and -30 °C and can be described by the following equation:

$$I_M(t) = A_{11} \exp(-\lambda_1 t) + A_{12} \exp(-\lambda_2 t) + A_{13} \exp(-\lambda_D t) \quad (1)$$

An approach by this equation leads to good fits, as can be seen from the quality of the error function and the χ^2 value.

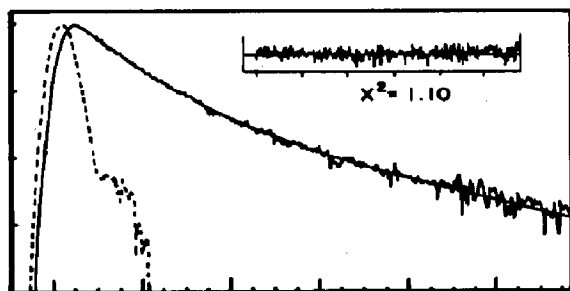


Fig. 7. Monomer (330 nm) decay curve of DNEME in iso-octane at -60 °C approached by a sum of three exponentials. The weighted residuals in units of σ (expected deviation) and the value for χ^2 are also shown.

Approach by a bi-exponential decay leads to large errors. Above -30°C , the decay curves can be analyzed by a bi-exponential approach:

$$I_M(t) = A_M \exp(-\lambda_M t) + A_{13} \exp(-\lambda_D t) \quad (2)$$

The time evolution of the excimer fluorescence can be approached by a

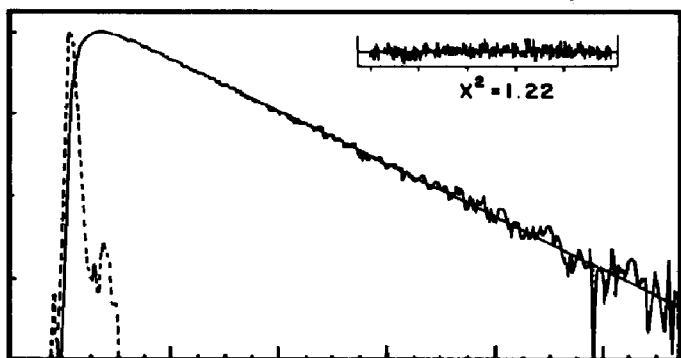


Fig. 8. Excimer (440 nm) decay curve of DNEME in iso-octane at -60°C approached by a difference of two exponentials. The weighted residuals in units of σ (expected deviation) and the value for χ^2 are also shown.

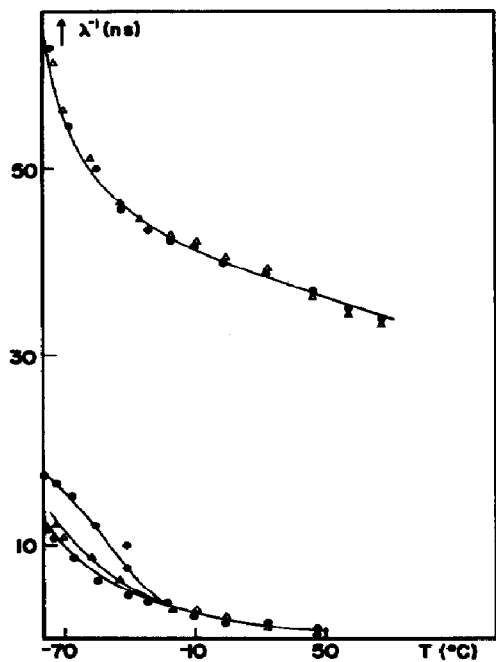


Fig. 9. Fluorescence decay parameters of DNEME in iso-octane: ●, monomer region; △, excimer region.

difference of two exponentials in the whole temperature range measured (Fig. 8):

$$I_D(t) = A_{21} \exp(-\lambda_{INC}t) + A_{22} \exp(-\lambda_D t) \quad (3)$$

with $A_{21} = -A_{22}$.

In Fig. 9, the decay parameters of the monomer fluorescence as well as those of the excimer fluorescence are plotted against temperature.

From Fig. 9 it is clear that the longest-living component in the monomer region corresponds to the decay of the excimer (λ_D^{-1}), indicating that this monomer component originates from dissociation of the excimer. This is further substantiated by the increasing contribution of this slowest-decaying component with increasing temperature, as shown by the evolution of the amplitude ratios in the monomer region with increasing temperature (Fig. 10). Furthermore, it is important to notice that between -80 and -30 °C the parameter related to the growing in of the excimer (λ_{INC}) lies in between λ_1 and λ_2 but equals λ_M above -30 °C.

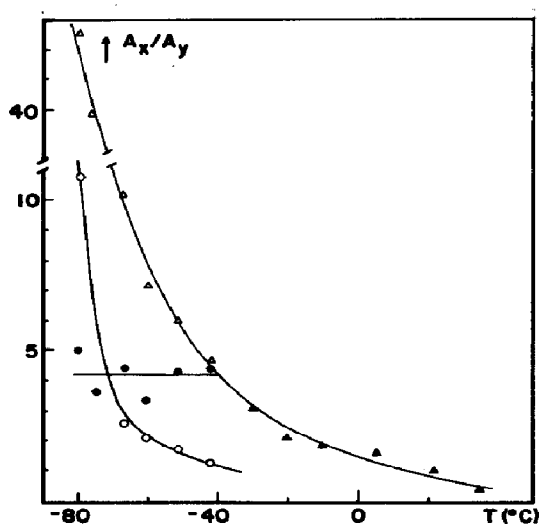
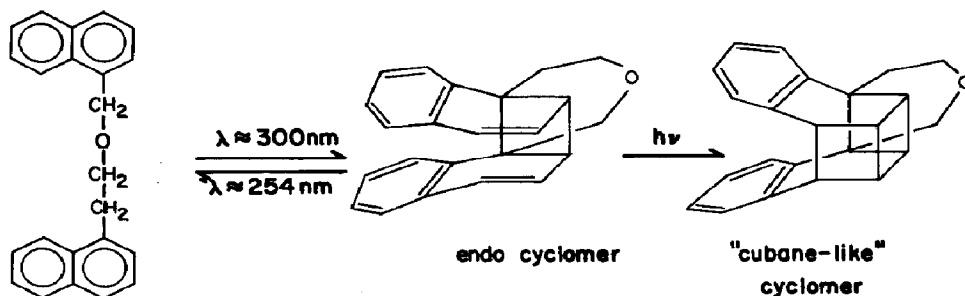


Fig. 10. Amplitude ratios A_{11}/A_{12} (●), A_{11}/A_{13} (△), A_{12}/A_{13} (○) and A_M/A_{13} (▲) for the monomer region vs. temperature.

3.5. Photocyclomerization

Unlike DNME [4], where both endo and exo cyclomers were formed, irradiation of DNEME with $\lambda \geq 300$ nm yielded only endo cyclomer, which could be converted under prolonged irradiation to a "cubane-like" cyclomer [7]. Sensitization with benzophenone [25] yielded no reaction, proving that the endo cyclomer is formed via the singlet excited state. In order to obtain more information about the reaction pathway, the endo cyclomer was cleaved with 254 nm light at 77 K in an ethanol matrix. Apart from the emission of the locally excited state of the naphthalene chromophore



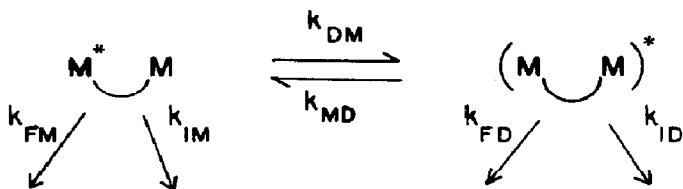
Scheme I.

of residual DNEME, an unstructured fluorescence with a maximum at 402 nm was observed from the frozen solutions after cleavage. This emission can clearly be ascribed to the endo excimer of DNEME. It may therefore be supposed that the cyclomerization proceeds via the endo excimer. Using molecular models it can easily be shown that in DNEME the formation of an exo excimer, comparable with that in DNME, with a parallel but shifted position of the two naphthyl groups, is prohibited by the severe steric hindrance induced by the $\text{CH}_2\text{-O-CH}_2\text{-CH}_2$ chain. The formation of an exo cyclomer via such an excimer is thus unlikely. An endo excimer, however, is possible, but with a slightly larger interchromophoric distance compared with DNME.

The quantum yield of cyclomerization was found to be 0.001 at room temperature.

3.6. Kinetic scheme

In Fig. 9 it can be seen that the decay parameters describing the excimer and monomer fluorescence coincide at temperatures higher than -20°C , indicating that the kinetic scheme for intramolecular excimer formation, proposed by Förster and elaborated by Klöpffer and Johnson [21 - 24], is valid in this region:



Scheme II.

In this scheme, k_{DM} is the rate constant of excimer formation while k_{MD} is that of excimer dissociation, k_{FM} is that of fluorescence from the locally excited state, k_{IM} is that of non-radiative decay from the locally excited state, k_{FD} is that of excimer fluorescence and k_{ID} is that of non-radiative decay from the excimer. Using the two decay parameters from $I_{\text{M}}(t)$, the ratio of the contribution of the fast decaying component to the contribution of the slower decaying component (A factor) and the model lifetime,

we can calculate all the kinetic parameters according to Förster's scheme. Whether the lifetime of NMME or NEME is used does not make any difference, as they nearly coincide in this temperature region, as can be seen from Fig. 2. The rate constants k_{DM} , k_{MD} and k_D are plotted against temperature in Fig. 11 and the values of E_{DM} , E_{MD} , E_D , ΔH and ΔS , obtained in iso-octane, are listed in Table 3, together with some values obtained earlier for DNME. In Table 4 values of k_{DM} , k_{MD} , k_D , $k_M(\text{NMME})$ and $k_M(\text{NEME})$ at various temperatures are summarized. It can be seen that k_D and k_M are always smaller than k_{MD} and k_{DM} and that k_D only slightly increases with increasing temperature. This explains the occurrence of an isoemissive point in the fluorescence spectra.

Using the rate constants obtained from the experiments under non-stationary conditions, we can calculate the quantum yields of monomer and excimer fluorescence according to

$$\phi_{FM} = \frac{k_{FM} Y}{XY - k_{DM} k_{MD}} \quad (4)$$

$$\phi_{FD} = \frac{k_{FD} k_{DM}}{XY - k_{DM} k_{MD}} \quad (5)$$

with $X = k_M + k_{DM}$ and $Y = k_D + k_{MD}$, and compare these with the values obtained in the stationary measurements.

In eqn. (5), k_{FD} is unknown. We calculated k_{FD} from the experimental ϕ_{FD} at one temperature and using this value we calculated ϕ_{FD} at other

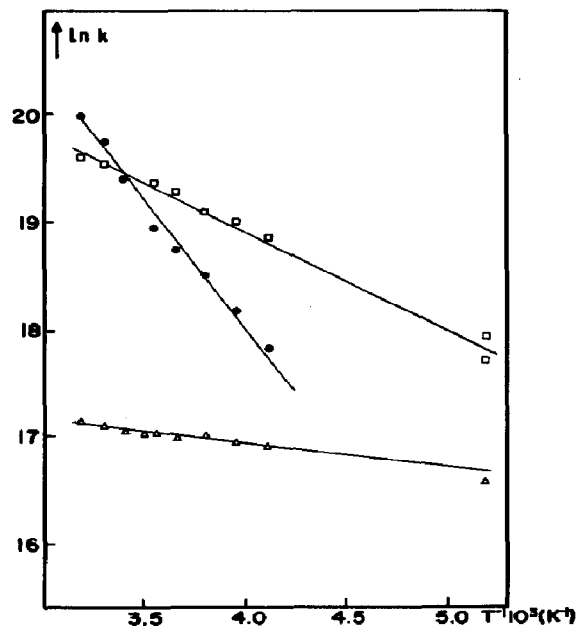


Fig. 11. Temperature dependence of k_{DM} (\square), k_{MD} (\bullet) and k_D (\triangle) for DNEME in iso-octane.

TABLE 3

Spectral, thermodynamic and kinetic properties of 2-(1-naphthyl)ethyl 1-naphthylmethyl ether compared with those of di(1-naphthylmethyl) ether [6] in iso-octane

Property	DNME	DNEME
λ_{\max} (nm)	413	398
FWHH (cm^{-1})	4450	4750
ϕ_{FM}	0.006	0.044
ϕ_{FD}	0.038	0.046
E_{DM} (kJ mol^{-1})	9, 11 ^a	6.5
ΔH (kJ mol^{-1})	-25 ^b	-15 ^b
	-15 ^c	
ΔS ($\text{J mol}^{-1} \text{K}$)		-50
E_{R} (kJ mol^{-1})		56
E_{D} (kJ mol^{-1})	26	1.7
k_{FD} (s^{-1})	6×10^6	2×10^6
k_{DM} (s^{-1})		3×10^8
k_{MD} (s^{-1})		4×10^8
k_{D} (s^{-1})	14×10^7	2×10^6
k_{T}^{d} (s^{-1})	3×10^6	5×10^4

FWHH, full width at half-height.

^a Values for fast and slow conformations respectively.

^b Obtained from the Stevens-Ban plot.

^c Obtained from single-photon counting data.

^d Obtained from $\phi_{\text{T}} k_{\text{FD}} / \phi_{\text{FD}} = k_{\text{T}}$ [31].

TABLE 4

Rate constants k_{DM} , k_{MD} and k_{D} of 2-(1-naphthyl)ethyl 1-naphthylmethyl ether and k_{M} of methyl 1-naphthylmethyl ether and methyl 2(1-naphthyl)ethyl ether in iso-octane at various temperatures

Temperature (°C)	$10^8 k_{\text{DM}}$ (s^{-1})	$10^8 k_{\text{MD}}$ (s^{-1})	$10^8 k_{\text{D}}$ (s^{-1})	$10^8 k_{\text{M}}$ (s^{-1})	
				NMME	NEME
-30	1.7	0.6	0.21	0.23	0.21
-10	2.0	1.1	0.23	0.24	0.22
+10	2.6	1.7	0.24	0.25	0.23
+30	3.1	3.8	0.26	0.26	0.24
+40	3.2	4.8	0.27	0.27	0.26

temperatures. As can be seen from Fig. 12 the calculated and experimental values of ϕ_{FM} and ϕ_{FD} match very well.

It remains to explain the occurrence of the tri-exponential decay in the monomer region from -70 to -40 °C. The slowest-decaying component in this region, λ_{D} , clearly originates from dissociation of the excimer as demonstrated earlier. In DNME it was assumed that two sets of conformations exist, differing in the relative orientation of the naphthyl groups and

the excimer and its repulsive ground state. (We are grateful to a referee for the suggestion of this scheme as an alternative explanation for the tri-exponential decay in the monomer region at lower temperatures.)

In both cases it is impossible to solve the different equations which describe the concentrations of excited monomers and excimers, as the excimer dissociates in the temperature region between -70 and -20 °C. Therefore we shall restrict ourselves to lower temperatures where excimer dissociation is negligible. Within the framework of the scheme, the rate constants k_F and k_S and the quantum yields ϕ_{FM} and ϕ_{FD} are described by

$$k_S = \lambda_2 - k_M \quad (6)$$

$$k_F = \lambda_1 - k_M \quad (7)$$

$$\phi_{FM} = k_{FM} \left\{ \frac{X_F}{k_M + k_F} + \frac{X_S}{k_M + k_S} \left(1 + \frac{k_S}{k_M + k_F} \right) \right\} \quad (8)$$

$$\phi_{FD} = \frac{k_{FD}k_F}{k_D(k_M + k_F)} \left(X_F + X_S \frac{k_S}{k_M + k_S} \right) \quad (9)$$

with

$$X_F = \frac{A_{12}k_S + A_{11}k_F}{(A_{12} + A_{11})k_F}$$

$$X_S = 1 - X_F$$

whereas if explanation (2) is valid, k_{DM} , ϕ_{FM} and ϕ_{FD} are given by

$$k_{DM} = \lambda_1 - k_{M(NMME)} \quad (10)$$

$$k_{DM} = \lambda_2 - k_{M(NEME)} \quad (11)$$

$$\phi_{FM} = X_{NMME} \left\{ \frac{k_{FM(NMME)}}{k_{DM} + k_{M(NMME)}} \right\} + X_{NEME} \left\{ \frac{k_{FM(NEME)}}{k_{DM} + k_{M(NEME)}} \right\} \quad (12)$$

$$\phi_{FD} = \frac{k_{FD}k_{DM}}{k_D} \left\{ \frac{X_{NMME}}{k_{DM} + k_{M(NMME)}} + \frac{X_{NEME}}{k_{DM} + k_{M(NEME)}} \right\} \quad (13)$$

with

$$X_{NMME} = \frac{A_{11}}{A_{11} + A_{12}}$$

and

$$X_{NEME} = \frac{A_{12}}{A_{11} + A_{12}}$$

However, it must be kept in mind that eqns. (6) - (9) only apply if it is assumed that $k_{-S} < k_F + k_M$, which is plausible at low temperatures [26].

If the occurrence of λ_1^{-1} and λ_2^{-2} is really related to the two different naphthalene moieties in DNEME, the same value for the rate constant of

excimer formation should be found at -80°C , where no excimer dissociation is observed, from either λ_1 or λ_2 , according to eqns. (10) and (11). The same value for k_{DM} , within experimental error, was obtained. Furthermore, this value is in agreement with that found on extrapolating $\ln k_{\text{DM}}$ versus $1/T$ to a temperature of -80°C (Fig. 11). However, if the scheme is valid, according to eqns. (6) and (7) comparable values for k_{F} and k_{S} are found, which means that the rate constant for interconversion between both groups of conformations is of the order of magnitude of formation of endo excimer from the set of F^* conformations, which is quite possible at this temperature [27]. The values of ϕ_{FM} and ϕ_{FD} can then be calculated according to eqns. (8) and (9) or (12) and (13). Both sets of equations yield the same values, within experimental error, and they match very well with the corresponding experimental values (Fig. 12). From the above it is clear that for the moment it is not possible to differentiate between the two alternative explanations for the lower temperature region. Also, the fact that λ_1^{-1} and λ_2^{-1} coincide above -20°C can be explained in both cases. Within the framework of the scheme this means that the interconversion between the two sets of conformations becomes so rapid on the time scale of excimer formation and dissociation that they do not show up as separate kinetic entities [27, 28], whereas for explanation (2) this is related to the fact that the lifetimes of the model compounds NMME and NEME become very similar (Fig. 2).

4. Discussion

The experimental data obtained from lifetime measurements indicate that the intramolecular excimer formation in DNEME can be described by Förster's scheme above temperatures of -20°C . The observation at lower temperatures of a tri-exponential decay in the monomer region can be explained by excimer dissociation, combined with either a different behavior of the two naphthyl moieties, $\alpha\text{-N-CH}_2\text{-O}$ and $\text{O-CH}_2\text{-CH}_2\text{-}\alpha\text{-N}$ or a kinetic scheme involving two consecutive sets of conformations. There is full compatibility between the ΔH values obtained from the Stevens-Ban plot and from the single-photon counting data. The obtained ΔS value of $-50 \text{ J K}^{-1} \text{ mol}^{-1}$ is in agreement with values reported for other bichromophoric systems [29, 30]. The dissociation of the excimer clearly shows up in both the fluorescence spectra and the $I_{\text{M}}(t)$ curves. Compared with DNME, the excimer of DNEME is characterized by a larger FWHH, a more hypsochromic λ_{max} , a smaller k_{FD} and k_{ID} and considerable dissociation to the locally excited state, as a result of the smaller stabilization energy. Similar results have been observed by De Schryver and coworkers [26] in a comparative study of the excimer properties of bis(9-(10-phenyl)anthryl)-methyl ether and bis(9-(10-phenyl)anthryl-methoxy)methane. The rate constant for photocyclomerization of DNEME is about 100 times smaller than that for DNME. Using molecular models it can easily be shown that

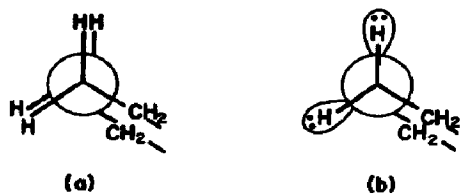


Fig. 13. Interactions in the chain in the excimer conformation of (a) DNB and (b) DNEME.

the path to a close-encounter geometry is governed by a much higher overall steric hindrance in DNEME than in DNME. Finally there seems to be a dramatic effect on intramolecular processes in replacing an oxygen atom by a methylene group. For DNB a negligible amount of excimer fluorescence is observed only at low temperatures [1], whereas for DNEME considerable excimer fluorescence is detected in the whole temperature region. The lack of excimer formation in DNB was explained by strong H-H repulsions in the linking butane chain in the excimer configuration (Fig. 13). In DNEME the hydrogen-free electron pair interactions are obviously much smaller.

Acknowledgments

Many thanks are due to Professor F. C. De Schryver for measurements on his single-photon counting equipment and for his helpful discussions. The research described was supported by the Office of Basic Energy Sciences of the Department of Energy. This is Document NDRL-2696 from the Notre Dame Radiation Laboratory.

References

- 1 E. A. Chandross and C. J. Dempster, *J. Am. Chem. Soc.*, **92** (1970) 3586; **92** (1970) 703.
- 2 Ph. Avouris, J. Kordas and M. Ashraf El-Bayoumi, *Chem. Phys. Lett.*, **26** (1974) 373.
- 3 M. Ashraf El-Bayoumi, *J. Phys. Chem.*, **80** (1976) 2259.
- 4 R. Todesco, J. Gelan, H. Martens, J. Put and F. C. De Schryver, *Tetrahedron Lett.*, **31** (1978) 2845.
- 5 R. Todesco, J. Gelan, H. Martens, J. Put and F. C. De Schryver, *Bull. Soc. Chim. Belg.*, **89** (1980) 521.
- 6 R. Todesco, J. Gelan, H. Martens, J. Put and F. C. De Schryver, *J. Am. Chem. Soc.*, **103** (1981) 7304.
- 7 R. Todesco, J. Gelan, H. Martens, J. Put and F. C. De Schryver, *Tetrahedron*, **39** (1983) 1407.
- 8 S. Ito, M. Yamamoto and Y. Nishijima, *Bull. Chem. Soc. Jpn.*, **54** (1981) 35.
- 9 H. Itagaki, A. Okamoto, K. Horie and I. Mita, *Chem. Phys. Lett.*, **78** (1981) 143.
- 10 K. Demeyer, M. Van der Auweraer, L. Aerts and F. C. De Schryver, *J. Chim. Phys.*, **77** (1980) 493.

- 11 F. C. De Schryver, K. Demeyer, M. Van der Auweraer and E. Quanten, *Ann. N.Y. Acad. Sci.*, **93** (1981) 366.
- 12 F. C. De Schryver, K. Demeyer and S. Topet, *Macromolecules*, **16** (1983) 89.
- 13 S. N. Semerak and C. W. Frank, *Adv. Polym. Sci.*, **54** (1984) 32, and references cited therein.
- 14 R. S. Davidson and T. D. Whelan, *J. Chem. Soc., Chem. Commun.*, (1977) 361.
- 15 M. Goldenberg, J. Emert and H. Morawetz, *J. Am. Chem. Soc.*, **100** (1978) 7171.
- 16 N. Boens, M. De Brackeleire, J. Huybrechts and F. C. De Schryver, *Z. Phys. Chem. (Wiesbaden)*, **101** (1976) 417.
- 17 J. B. Birks, in J. B. Birks (ed.), *Photophysics of Aromatic Molecules*, Wiley, London, 1970, p. 312.
- 18 B. L. Johnson and J. Smith, in M. B. Huglin (ed.), *Light Scattering from Polymer Solutions*, Academic Press, London, 1972, p. 27.
- 19 B. Stevens and M. I. Ban, *Trans. Faraday Soc.*, **60** (1964) 1515.
- 20 J. B. Birks and T. A. King, *Proc. R. Soc. (London), Ser. A*, **291** (1966) 244.
- 21 W. Klöpffer, in J. B. Birks (ed.), *Organic Molecular Photophysics*, Vol. I, Wiley, London, 1973, p. 357.
- 22 J. B. Birks, in J. B. Birks (ed.), *Photophysics of Aromatic Molecules*, Wiley, London, 1970, p. 301.
- 23 W. Klöpffer and W. Lipty, *Z. Naturforsch.*, **25a** (1970) 1091.
- 24 G. E. Johnson, *J. Chem. Phys.*, **61** (1974) 3002; **63** (1975) 4047.
- 25 C. A. Parker, in C. A. Parker (ed.), *Photoluminescence of Solutions*, Elsevier, Amsterdam, 1968, p. 92.
- 26 M. Van der Auweraer, A. Gilbert and F. C. De Schryver, *J. Am. Chem. Soc.*, **102** (1980) 4007.
- 27 R. M. Levy, M. Karplus and J. A. McCommon, *Chem. Phys. Lett.*, **65** (1979) 4.
- 28 K. A. Zachariasse, G. Duveneck and W. Kühnle, *Chem. Phys. Lett.*, **113** (1985) 337.
- 29 F. C. De Schryver, K. Demeyer, J. Huybrechts, H. Bouas-Laurent and A. Castellan, *J. Photochem.*, **20** (1982) 341.
- 30 K. A. Zachariasse, W. Kühnle and A. Weller, *Chem. Phys. Lett.*, **59** (1978) 375.
- 31 J. B. Aladekomo, *J. Lumin.*, **6** (1973) 83.